Heat Shock Protein 90 Inhibition in Imatinib-Resistant Gastrointestinal Stromal Tumor

Sebastian Bauer,[1] Lynn K. Yu,[1] George D. Demetri,[2,3] and Jonathan A. Fletcher[1,2]

[1]Department of Pathology, Brigham and Women's Hospital, [2]Center for Sarcoma and Bone Oncology, Dana-Farber Cancer Institute, and [3]Ludwig Center at Dana Farber/Harvard Cancer Center, Boston, Massachusetts

Abstract

Inhibition of KIT oncoproteins by imatinib induces clinical responses in most gastrointestinal stromal tumor (GIST) patients. However, many patients develop imatinib resistance due to secondary KIT mutations. Heat shock protein 90 (HSP90) protects KIT oncoproteins from proteasome-mediated degradation, and we therefore did preclinical validations of the HSP90 inhibitor, 17-allylamino-18-demethoxy-geldanamycin (17-AAG), in an imatinib-sensitive GIST cell line (GIST882) and in novel imatinib-resistant GIST lines that are either dependent on (GIST430 and GIST48) or independent of (GIST62) KIT oncoproteins. 17AAG (>100 nmol/L) inhibited imatinib-sensitive and imatinib-resistant KIT oncoproteins, with substantially reduced phospho-KIT and total KIT expression after 30 minutes and 6 hours, respectively. KIT signaling intermediates, including AKT and mitogen-activated protein kinase, were inactivated by 17-AAG in the KIT-positive GIST lines, but not in the KIT-negative GIST62. Likewise, cell proliferation and survival were inhibited in the KIT-positive GISTs but not in GIST62. These findings suggest that 17-AAG biological effects in KIT-positive GISTs result mainly from KIT oncoprotein inhibition. The dramatic inactivation of imatinib-resistant KIT oncoproteins suggests that HSP90 inhibition provides a therapeutic solution to the challenge of heterogeneous imatinib resistance mutations in GIST patients. (Cancer Res 2006; 66(18): 9153-61)

Introduction

Gastrointestinal stromal tumors (GIST) are the most frequent type of gastrointestinal mesenchymal tumor, and they have been refractory to conventional chemotherapy, with a median survival of only 12 to 19 months in patients with unresectable or metastatic disease (1). However, rapid progress in the treatment of GIST was made after the discovery that *KIT* and *PDGFRA* gain-of-function mutations are present in >90% of GISTs (2, 3). Therapeutic inhibition of KIT or PDGFRA by the small-molecule inhibitor imatinib gives objective responses in ~50% of patients, with a median remission duration of >2 years and a median survival not reached after 2 years (4).

Despite the therapeutic success of imatinib, some patients express KIT or PDGFRA oncoproteins that are resistant to imatinib-mediated inhibition (4, 5). And although many GIST patients respond to imatinib, initially, they often manifest secondary, imatinib-resistant mutations within 2 to 5 years after starting therapy. Such patients can develop progressing lesions at multiple metastatic sites, and each of the metastases, within a given patient, can have a genomic mutational resistance mechanism that differs from the other metastatic sites in that patient (6–9). Although novel small-molecule KIT kinase inhibitors have been clinically tested, none of these drugs, which are essentially imatinib alternatives, are effective in inhibiting all the known imatinib resistance mutations (10–12). Salvage treatments for progressive disease following imatinib treatment show clinical benefit in a minority of patients and median survival after progression is only 15 months (11). Therefore, it is essential to validate novel therapeutic strategies that can address the inevitable problem of imatinib resistance in GIST patients irrespective of the specific mutational activation mechanisms. One such strategy is to enhance the cellular degradation of constitutively activated KIT oncoproteins, which might be accomplished by facilitating ubiquitination/proteasome–mediated oncoprotein processing. Recently, Fumo et al. (13) showed that KIT activation depends on protein stabilization by heat shock protein 90 (HSP90), with HSP90 inhibition causing degradation of wild-type KIT and an imatinib-resistant KIT D816V mutant.

17-Allylamino-18-demethoxy-geldanamycin (17-AAG) is a geldanamycin derivative (14, 15) that binds a conserved pocket in the HSP90 NH_2-terminal domain and prevents HSP90 from stabilizing client proteins. HSP90 client proteins are then increasingly directed towards the proteasome machinery for degradation (16, 17). There are more than 100 known HSP90 client proteins, and many of these, such as KIT, serve oncogenic roles, making HSP90 an attractive therapeutic target in various human cancers (18). 17-AAG has antitumor activity in breast cancer, prostate cancer, myeloma, and melanoma models (19–22), and phase I trials show only minor toxicities (23). Nonetheless, clinical applications have been hampered by the insolubility of 17-AAG, which has required formulations containing either DMSO/egg phospholipids or cremaphor, which are associated with unwanted side effects.

We hypothesized that HSP90 inhibition might provide a broadly relevant salvage option in GISTs progressing on imatinib therapy. This premise is based on the observation that most progressing GISTs contain secondary *KIT* resistance mutations, together with the pre-imatinib *KIT* primary oncogenic mutation, and the crucial KIT oncoprotein in these tumors therefore remains strongly activated and subject possibly to HSP90-mediated protection from proteasomal degradation. According to this hypothesis, HSP90 inhibition might induce KIT oncoprotein degradation irrespective of the genomic activating mutations in the oncoprotein. The studies reported herein validate this hypothesis by comparing effects of HSP90 inhibition in imatinib-sensitive and imatinib-resistant GIST models.

Requests for reprints: Sebastian Bauer, Department of Internal Medicine (Cancer Research), West German Cancer Center, University of Essen, Hufelandstraße 55, 45122 Essen, Germany. Phone: 49-201-723-3120; Fax: 49-201-723-2735; E-mail: sebastianbauer@uni-essen.de or Jonathan Fletcher, Department of Pathology, Brigham and Women's Hospital, 75 Francis Street, Boston, MA 02155. Phone: 617-732-5152; Fax: 617-278-6913; E-mail: jfletcher@partners.org.

doi:10.1158/0008-5472.CAN-06-0165

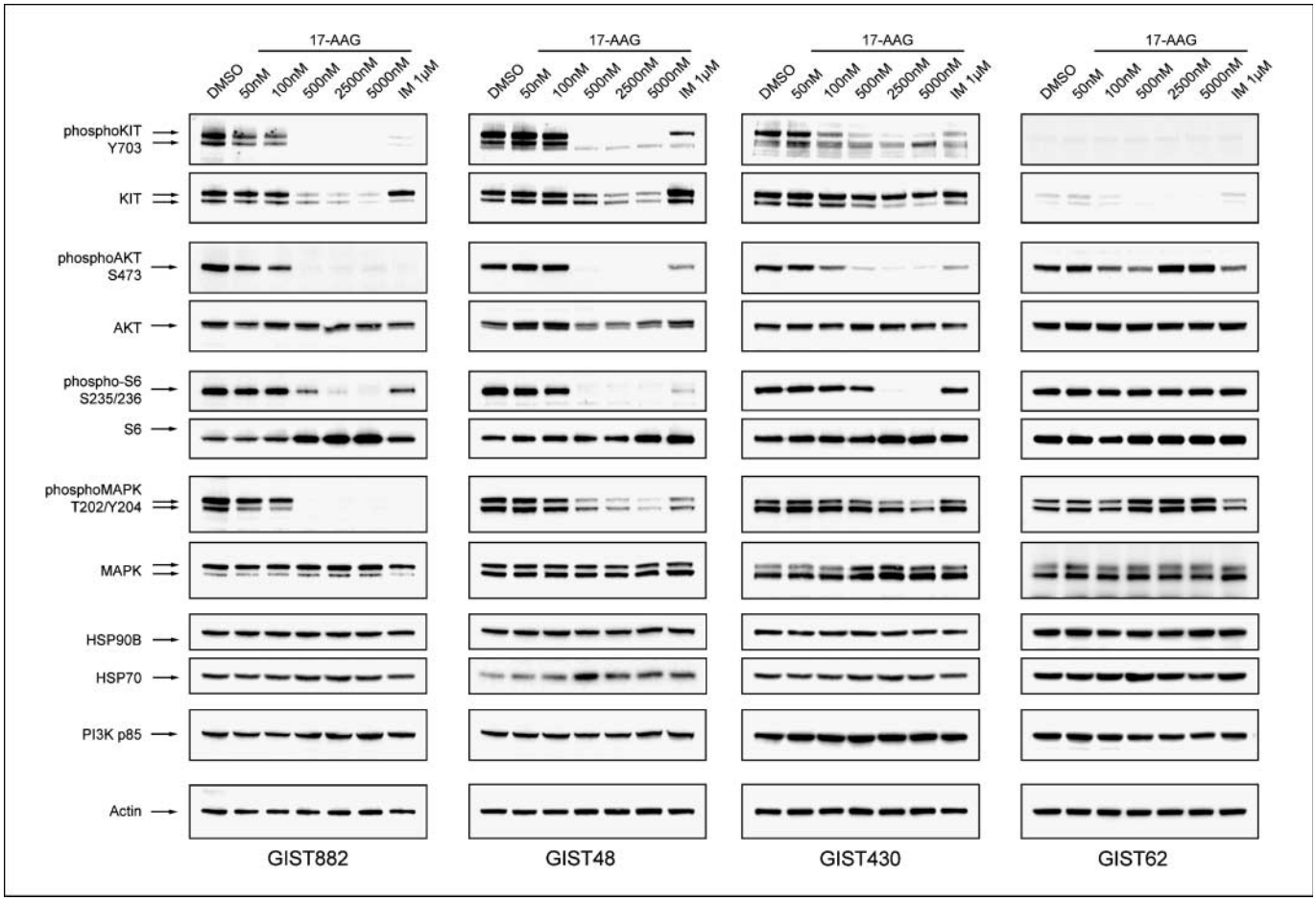

Figure 1. Immunoblotting for KIT, AKT, S6, MAPK, and HSP after 6 hours of 17-AAG or imatinib (*IM*) treatment in imatinib-sensitive (GIST882) and imatinib-resistant (GIST48, GIST430, and GIST62) cells. PI3K and actin stains serve as indicators of comparable loading.

Materials and Methods

Cell lines. GIST882, as previously described, was established from an untreated human GIST with an homozygous missense mutation in KIT exon 13, encoding a K642E mutant KIT oncoprotein (24). GIST430 and GIST48 were established from GISTs that had progressed, after initial clinical response, during imatinib therapy. GIST430 has a heterozygous primary *KIT* exon 11 (juxtamembrane region) in-frame deletion, accompanied by a heterozygous secondary exon 13 (kinase ATP-binding region) missense mutation (V654A). GIST48 has a primary, homozygous exon 11 missense mutation (V560D) and a heterozygous secondary exon 17 (kinase activation loop) mutation (D820A). GIST62 was derived from an untreated KIT-positive GIST with *KIT* exon 11 in-frame mutation, but the cell line, despite retaining the activating *KIT* mutation in all cells, expresses KIT transcript (data not shown) and protein at essentially undetectable levels (12). EWS502 was established from a human Ewing's sarcoma and expresses KIT strongly but lacks a *KIT* oncogenic mutation.

Reagents. The KIT inhibitor (imatinib mesylate) was provided by Novartis Pharma (Basel, Switzerland). 17-AAG and stem cell factor (SCF) were from Sigma-Aldrich (St. Louis, MO).

A rabbit polyclonal antibody to KIT was from DAKO (Carpinteria, CA). Monoclonal antibody to HSP90B and polyclonal rabbit antibodies to phospho-KIT Y703 and total p42/44 mitogen-activated protein kinase (MAPK) were from Zymed Laboratories (South San Francisco, CA). Monoclonal antibody to phosphatidylinositol 3-kinase (PI3K) p100α and polyclonal rabbit antibodies to phospho-p44/42 MAPK T202/Y204, phospho-AKT S473, total AKT, phospho-S6 Ser235/236, total S6, phospho-4E-BP1 Ser65, and phospho-PKCδ/θ (Ser643/676) were from Cell Signaling (Beverly, MA). Monoclonal antibodies for HSP70 and ubiquitin and a polyclonal antibody to PKCθ were from Santa Cruz Biotechnology (Santa Cruz, CA) and a polyclonal antibody to PI3K p85 was from Upstate Biotechnology (Lake Placid, NY).

***In vitro* assays.** Viability studies were carried out using the CellTiter-Glo luminescent assay (Promega, Madison, WI), in which the luciferase-catalyzed luciferin/ATP reaction provides an indicator of cell number (25). For these studies, the cell lines were plated at 15 to 40,000 cells per well in a 96-well flat-bottomed plate (Falcon, Lincoln, NJ), cultured in serum-containing media for 1 to 3 days, and then incubated for 72 hours with HSP90 or KIT inhibitors or DMSO-only solvent control. The CellTiter-Glo assay luminescence was measured with a Veritas Microplate Luminometer (Turner Biosystems, Sunnyvale, CA) and the data were normalized to the DMSO-only control group. All experimental points were measured in triplicate wells for each plate and were replicated in at least two plates.

Apoptosis studies were done by measuring caspase-3 and caspase-7 activation with the Caspase-Glo 3/7 Assay Kit (Promega). This assay uses a proluminescent substrate containing the DEVD sequence recognized and activated by caspase-3 and caspase-7 (26, 27) and the luminescence signal is proportional to net caspase-3 and caspase-7 activation (28). The experimental conditions were as described above for the CellTiter-Glo studies.

Western blotting and immunoprecipitation. Protein lysates were prepared from cell line monolayers according to standard protocols (29). Protein concentrations were determined with the Bio-Rad Protein Assay (Bio-Rad Laboratories, Hercules, CA). Electrophoresis and immunoblotting were carried out as previously described (30). KIT immunoprecipitations were done with a mouse monoclonal antibody (Santa Cruz Biotechnology) and Sepharose-protein G beads (Zymed Laboratories).

Cell cycle analysis. Cells were plated in six-well plates, grown until 80% confluence, and then treated for 24 to 72 hours with DMSO, 17-AAG (500 nmol/L), or imatinib (1 μmol/L). Cells were then trypsinized, washed thrice with HBSS, and stained with 4′,6-diamidino-2-phenylindole (DAPI; Nuclear isolation and staining solution, NPE Systems, Pembrooke Pines, FL) followed immediately by flow cytometric analysis (NPE Quanta, NPE Systems). Modfit LT software 3.1 (Verity Software House, Topsham, ME) was used for data analysis.

Analysis of nuclear fragmentation. GIST cell lines were grown to 25% to 50% confluence on chamber slides and then treated with DMSO, imatinib (1 μmol/L), or 17-AAG (1 μmol/L) for 48 hours. The cells were then washed with HBSS, fixed with 4% paraformaldehyde, and stained with DAPI. Nuclear fragmentation was then quantitated in at least 400 nuclei for each cell line.

Results

HSP90 inhibition and KIT signaling in GIST. Immunoblotting studies of KIT and downstream signaling protein activation were done by incubating confluent cells with media containing 17-AAG or imatinib for 6 hours. HSP90 inhibition by 17-AAG resulted in a dose-dependent decrease in KIT activation (as measured by Y703 phosphorylation) in KIT-positive cell lines GIST882, GIST48, and GIST430 (Fig. 1). IC_{50}s for inhibition of mature 160-kDa KIT tyrosine phosphorylation, at 6 hours, were between 100 and 200 nmol/L irrespective of whether the cells were imatinib sensitive (GIST882) or imatinib resistant (GIST48 and GIST430). Total KIT expression was decreased in these cell lines after 6 hours of 17-AAG treatment. 17-AAG inhibited expression of both mature and immature (145 kDa) KIT forms in GIST882 and GIST48, whereas expression of only the immature KIT form was substantially inhibited in GIST430 (Fig. 1).

Notably, KIT, AKT, and S6 were completely inactivated by >500 nmol/L 17-AAG in GIST882, GIST48, and GIST430, whereas imatinib treatment did not fully inactivate KIT in GIST430 or GIST48 and, accordingly, did not fully inactivate AKT and S6 (Fig. 1). By contrast, 17-AAG treatment of KIT-negative GIST62 did not inactivate AKT, S6, or MAPK (Fig. 1), suggesting that the 17-AAG signaling effects in GIST882, GIST48, and GIST430 were KIT dependent. Indeed, in GIST62, AKT and MAPK phosphorylation actually increased with 17-AAG doses of >500 nmol/L.

HSP90 inhibition and PI3K/KIT interactions in GIST. HSP90 inhibitor effects on KIT protein-protein interactions were evaluated in KIT immunoprecipitates after treating GIST882 and GIST48 with 17-AAG or imatinib mesylate for 6 hours. Interactions between KIT and the regulatory (p85) and catalytic (p110) PI3K subunits were inhibited in parallel with inhibition of activated KIT (Fig. 2). Likewise, interactions between KIT and HSP90β were inhibited commensurately with loss of KIT activation and expression. These findings confirm that 17-AAG inhibits HSP90 interaction with tyrosine phosphorylated KIT oncoproteins.

HSP90 inhibition and KIT signaling: time course studies. The dynamics of 17-AAG-mediated KIT inhibition were determined in a time course experiment where GIST882 was treated with 500 nmol/L 17-AAG for 6 hours. KIT activation was inhibited by 70% at 30 minutes, with nearly 100% inhibition at 60 minutes. KIT and AKT were inactivated before KIT degradation, which was not demonstrable until 6 hours of 17-AAG treatment (Fig. 3*A*). Likewise, KIT-PI3K complexing persisted after KIT inactivation, with, for example, 20% of the baseline level of PI3K coprecipitate evident after 6 hours of 17-AAG treatment (Fig. 3*B*). KIT ubiquitination decreased by 70% after 6 hours of 17-AAG treatment, in keeping with the decrease in total KIT expression.

HSP90 inhibition effects on wild-type KIT. The effects of HSP90 inhibition on wild-type KIT were evaluated by 17-AAG treatment of EWS502 cells. KIT expression was inhibited by 20% in EWS502 at 6 hours, compared with 80% inhibition in GIST882 (Fig. 4*A*). Likewise, expression of activated AKT inhibition was inhibited by 50% at 6 hours in EWS502, compared with 100% inhibition in GIST882. HSP90 expression was unaffected by 17-AAG treatment whereas HSP70 expression increased 2-fold.

HSP90 inhibitor effects on activated wild-type KIT were evaluated in EWS502 cells exposed to 100 ng of SCF and 1 μmol/L 17-AAG for 10, 30, or 60 minutes. KIT activation (phospho-KIT) was maximal after 10 minutes of SCF treatment and was not reduced by concurrent treatment with 17-AAG (Fig. 4*B*). KIT activation, after SCF stimulation alone, was short-lived, being undetectable after 30 and 60 minutes (Fig. 4*B*). Total KIT expression was reduced by 40% at 60 minutes after SCF treatment alone, and this reduction was not increased by concurrent treatment with 17-AAG. Given these marked SCF (100 ng/mL) effects on KIT expression, further EWS502 studies were done at lower doses of SCF with and without 17AAG treatment. Using an approach similar to that reported by

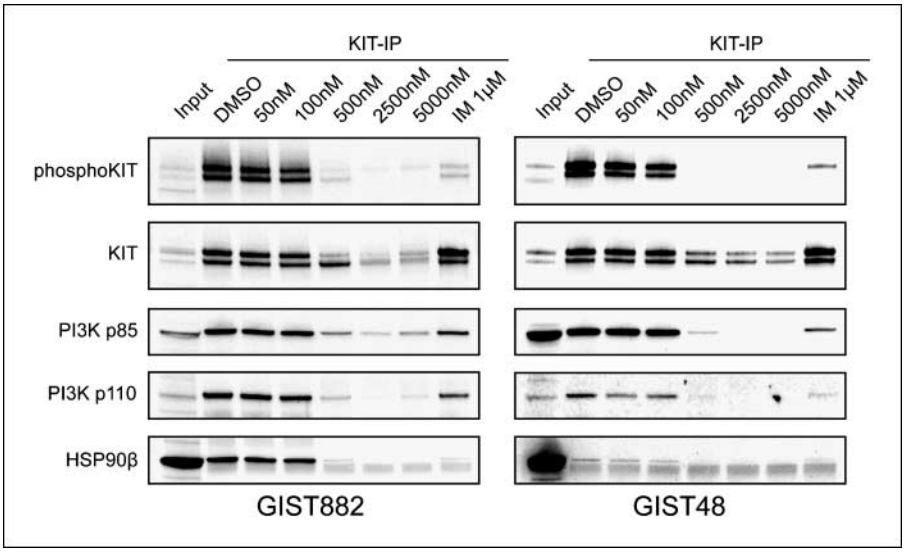

Figure 2. KIT immunoprecipitates of 17-AAG-treated (same doses as in Fig. 1) and imatinib-treated GIST cells were immunoblotted to evaluate KIT activation, KIT interactions with PI3K catalytic and regulatory components, and KIT interactions with HSP90.

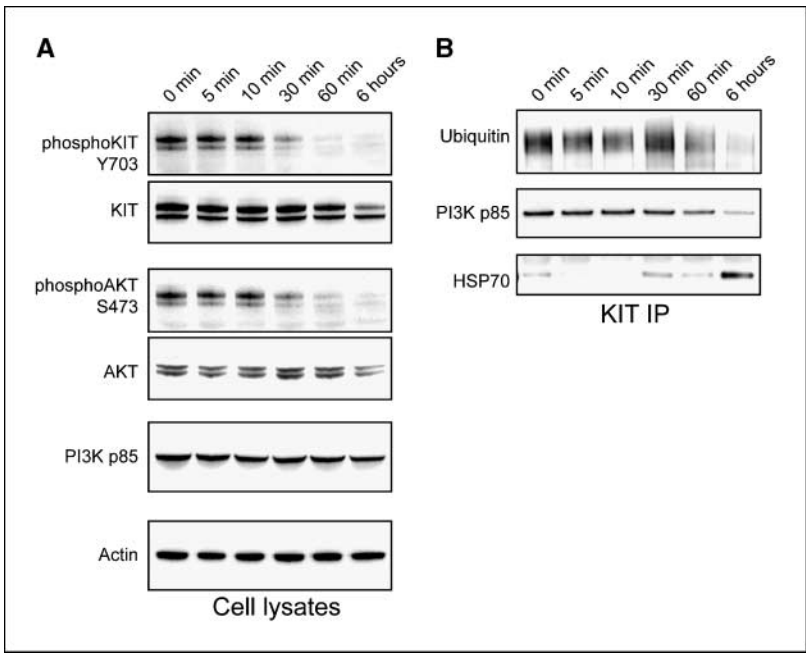

Figure 3. Time course study of GIST882 cells treated with 500 nmol/L 17-AAG. *A,* cell lysate immunoblots show onset of KIT and AKT inactivation, with PI3K and actin as loading controls. *B,* KIT immunoprecipitates show KIT ubiquitination and KIT interactions with PI3K and HSP70.

Fumo et al. (13), EWS502 cells were pretreated with SCF for 30 minutes, followed by treatment with 1 μmol/L 17-AAG for 6 hours. SCF treatment strongly inhibited total KIT expression, with 15%, 75%, and 89% inhibition after treatment with SCF at concentrations of 1, 10, and 100 ng/mL, respectively. SCF treatment combined with 17-AAG gave similar results, in that total KIT expression was inhibited by 45%, 82%, and 91% after treatment with SCF at concentrations of 1, 10, and 100 ng/mL, respectively (Fig. 4*C*).

In contrast to the EWS502 findings, 17AAG fully inactivated KIT after 60 minutes in GIST882, accompanied by 58% reduction in the expression of both immature and mature KIT. Combined treatment with SCF and 17AAG reduced total KIT expression in GIST882, comparable to that achieved with 17AAG treatment alone (Fig. 4*C*).

Comparative effects of HSP90 inhibition versus imatinib on GIST proliferation. To determine 17-AAG effects on cell proliferation, GIST cells were treated with increasing concentrations of 17-AAG alone and with imatinib (0.1 and 1 μmol/L) for 3 days. All KIT-expressing cell lines showed inhibition of cell proliferation at 100 nmol/L 17-AAG (Fig. 5). IC_{50}s for proliferation at day 3 were 130 nmol/L for GIST48 and 220 nmol/L for GIST430 (Fig. 5*A*). By contrast, the proliferation IC_{50} was not reached in KIT-negative GIST62 cells, which had only 19% inhibition of proliferation at 2,500 nmol/L 17-AAG (Fig. 5*A*). GIST882 cells showed a delayed antiproliferative effect, with an IC_{50} of 3,100 nmol/L at day 3 (Fig. 5*A*), despite complete inhibition of phospho-KIT by 500 nmol/L 17-AAG, but with an IC_{50} of 330 nmol/L at day 6 (Fig. 5*B*). Additive antiproliferative effects for the combination of 17-AAG and imatinib were not observed in any of the GIST cell lines (Fig. 5). However, the combination of 1 μmol/L imatinib and 50 to 2,500 nmol/L 17-AAG showed antagonistic effects in GIST882 at day 3 (Fig. 5*A*). This antagonistic effect disappeared by day 6 of combined imatinib and 17-AAG treatment (Fig. 5*B*).

Comparative effects of HSP90 inhibition versus imatinib on GIST apoptotic activity. Imatinib induced substantial caspase-3/caspase-7 activation in GIST882 but not in GIST430, GIST48, and GIST62, whereas 17-AAG induced caspase activation in all GIST lines (Fig. 6*A*). Combined treatment with imatinib and 17-AAG was not synergistic with respect to caspase activation in any of the GIST lines, although a small additive effect was seen with 17-AAG and 1 μmol/L imatinib in GIST48 (Fig. 6*A*). GIST882 apoptotic response, as indicated by sub-G_1 phase nuclear fragmentation, peaked at 48 hours and was 0% in the DMSO control, 26% after imatinib, and 11% after 17-AAG treatment (Fig. 6*B*). By contrast, the GIST48 (imatinib-resistant) sub-G_1 nuclear fragmentation peaked at 24 hours and was 1% in the DMSO control, 11% after imatinib, and 40% after 17-AAG treatment (Fig. 6*B*). DAPI staining analyses for nuclear fragmentation (Fig. 6*C* and *D*) of GIST882 cells showed 23% and 21% apoptotic cells after 48-hour incubation with imatinib and 17-AAG, respectively (Fig. 6*C*). By contrast, apoptotic nuclear fragmentation in the imatinib-resistant GIST430 and GIST48 lines was 10-fold higher after 17-AAG treatment than after imatinib treatment (Fig. 6*C* and *D*).

Comparative effects of HSP90 inhibition versus imatinib on GIST cell cycle activity. 17-AAG and imatinib cell cycle effects were evaluated in GIST882 and GIST48 cells treated with DMSO, imatinib (1 μmol/L), and 17-AAG (500 nmol/L). The S-phase peak in GIST882 was reduced after 24 hours and was nearly inapparent at 48 hours after imatinib and 17-AAG treatment (Fig. 6*B*). The G_1-G_0 peak in GIST882 increased from 79% in control (DMSO-only) cells to 87% in both imatinib- and 17-AAG-treated cells, consistent with a G_1 block.

Discussion

Activating mutations of the KIT and PDGFRA receptor tyrosine kinases are early, and even initiating, oncogenic events in most GISTs, and they continue to play essential transforming roles in GISTs that have progressed to malignancy (31). Biochemical KIT inhibition by imatinib induces dramatic clinical responses; however, patients often develop secondary imatinib-resistant mutations, which are responsible for clinical progression. Because most imatinib-resistant, progressing GISTs express strongly activated KIT, it can be assumed that KIT oncoproteins remain a

useful therapeutic target at the time of clinical progression (6). Therefore, strategies to overcome imatinib resistance have focused on inhibition of KIT oncoproteins and KIT-dependent signaling intermediates (11, 32).

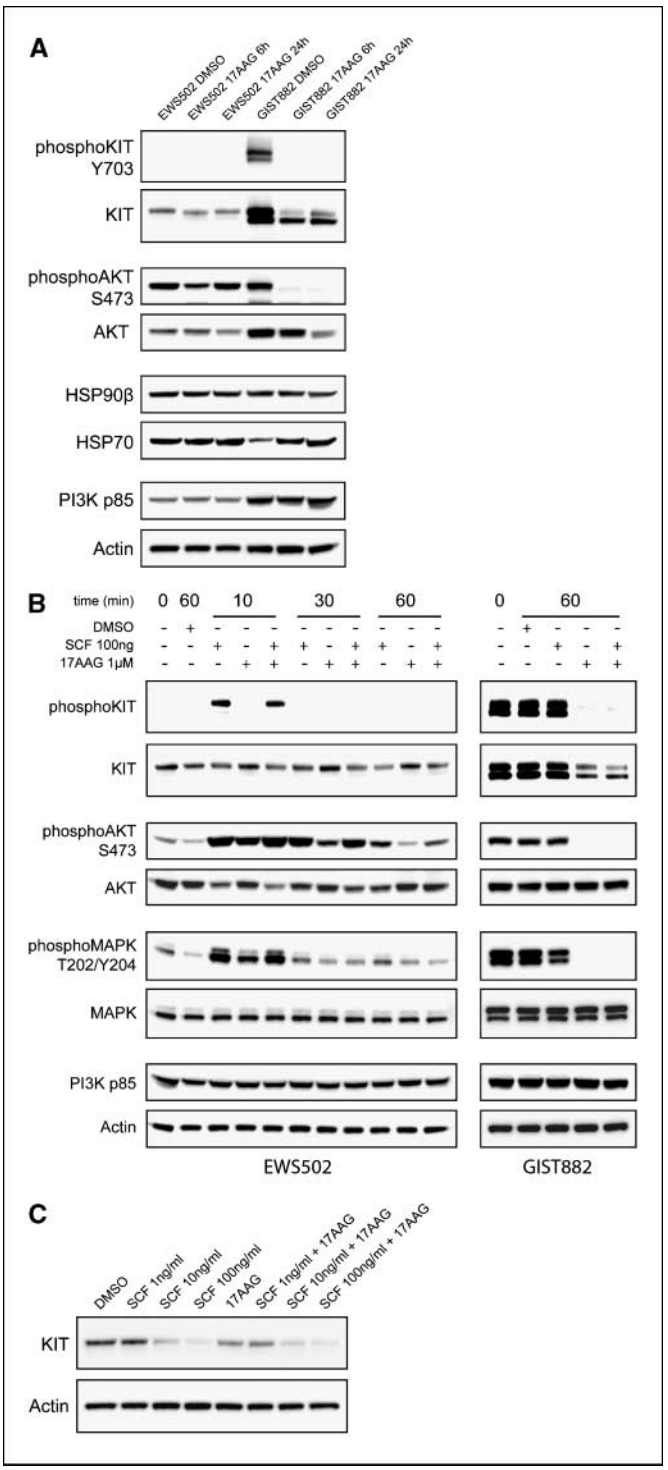

Figure 4. *A,* immunoblotting for KIT, AKT, and HSP after treatment of EWS502 and GIST882 cells with 1 μmol/L 17-AAG. PI3K and actin serve as loading controls. *B,* immunoblotting for KIT, AKT, and MAPK after EWS502 and GIST882 treatment with SCF (100 ng/mL) and 17-AAG (1 μmol/L), alone and in combination. *C,* immunoblotting for KIT expression after SCF dose-response study in EWS502 cells (+/− 17-AAG). Cells were pretreated with 1 to 100 ng/mL SCF for 30 minutes, followed by 1 μmol/L 17-AAG for 6 hours.

Although secondary mutations in the KIT kinase domain are found in most imatinib-resistant GISTs, these mutations are heterogeneous and can vary even between different progressing metastases in each patient (7). None of the novel small-molecule KIT kinase inhibitors, which typically bind to the kinase domain, are effective in inhibiting all the known imatinib resistance mutations (10–12). Hence, alternative therapeutic strategies are needed to overcome the problem of resistance to KIT kinase inhibitors. Recently, Fumo et al. (13) validated HSP90 as a therapeutic target in a mastocytosis cell line with imatinib-resistant KIT oncogenic mutation. HSP90 inhibition by 17-AAG destabilized KIT and led to rapid degradation of the imatinib-resistant KIT mutant, D816V. The data reported herein are the first to show that 17-AAG inactivates KIT oncoproteins with secondary imatinib-resistant mutations in GIST. These studies suggest that HSP90 inhibition might be clinically effective in imatinib-resistant GISTs irrespective of the exact type of secondary KIT mutation.

By evaluating 17-AAG effects in four GIST cell lines, we show that HSP90 chaperone functions are crucial for expression of oncogenic KIT. IC_{50}s for KIT-phosphorylation after 6 hours were 100 to 200 nmol/L in all cell lines and near complete inhibition was observed at 500 nmol/L (Fig. 1). Notably, HSP90 inhibition resulted in substantially reduced KIT expression in imatinib-sensitive (GIST882) and imatinib-resistant (GIST48 and GIST430) cell lines. These data are in keeping with those of Fumo et al. (13) in mastocytosis, where KIT inhibitory effects were seen at 17-AAG doses of >100 nmol/L. The clinical relevance of these findings is underscored by the fact that 17-AAG concentrations in the 1 μmol/L range are achievable in patients.

Interestingly, the KIT degradation resulting from 17-AAG treatment in the imatinib-resistant GIST430 cells affected disproportionately the immature, poorly glycosylated 145-kDa KIT proteins. There are several scenarios that might account for this selective degradation. First, HSP90 subcellular localization in some tumor cells might dictate that its interactions are preferentially with the endoplasmic reticulum–associated immature kinase rather than the membrane-associated mature kinase. Second, the immature oncogenic kinase might be more strongly activated in some GISTs and more dependent on HSP90 chaperone functions. Whatever the explanation, our findings indicate that HSP90 interactions with mature and immature KIT forms can vary between different GIST cell lines. Notably, GIST430 contains heterozygous *KIT* mutations and it is expected that half of the expressed KIT is oncogenic, with the other half being wild type. By contrast, GIST882 and GIST48 contain homozygous *KIT* mutations and express only oncogenic KIT. Therefore, it is possible that oncogenic KIT is chaperoned by HSP90, irrespective of the KIT glycosylation status, whereas activated wild-type KIT might be chaperoned preferentially by HSP90 in its immature, poorly glycosylated state. Alternately, mutant KIT might be overrepresented among the immature KIT population in GIST430 cells and might thereby be degraded preferentially by HSP90 inhibition.

HSP90 inhibitor effects on KIT oncogenic signaling were similar to those resulting from imatinib-mediated KIT biochemical inactivation in GISTs (Fig. 1). However, 17-AAG was more potent than imatinib in the GIST48 and GIST430 cell lines, with stronger inactivation of AKT, S6, and MAPK with 500 nmol/L 17-AAG than with 1 μmol/L imatinib. By contrast, HSP90 inhibition did not inactivate signaling intermediates in the KIT-negative GIST62 cell line. These findings suggest that 17-AAG inhibition of AKT, S6, and MAPK is KIT dependent in the GIST882, GIST430, and GIST48 cell

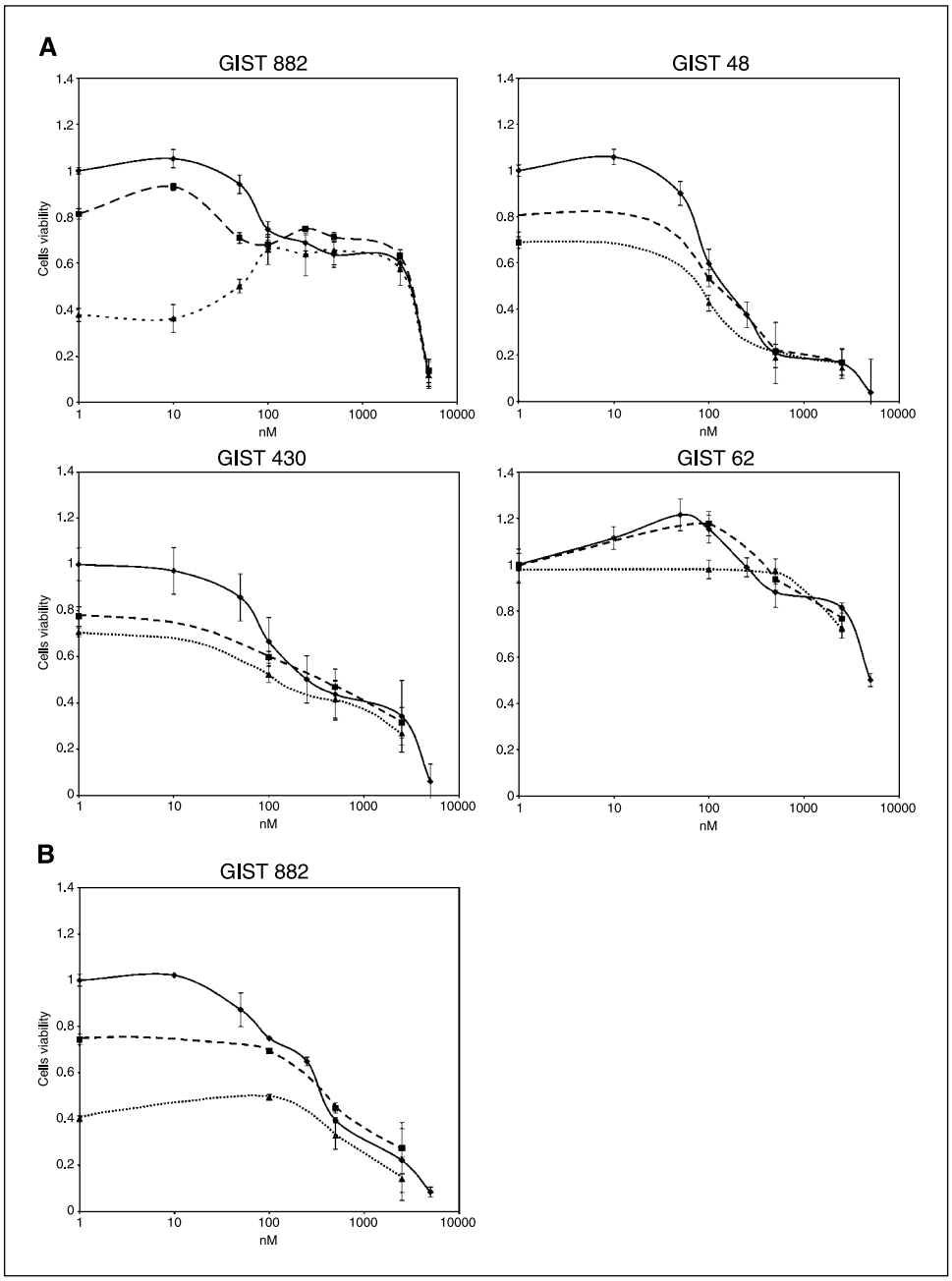

Figure 5. *A,* CellTiter-Glo ATP-based proliferation assays in imatinib-sensitive (GIST882) and imatinib-resistant GIST cell lines after treatment with 17-AAG alone versus 17-AAG in combination with 0.1 or 1 μmol/L imatinib. All cells were assessed after 3 days of treatment, with the data normalized to DMSO-only controls. *Points,* mean of quadruplicate cultures; *bars,* SD. *B,* proliferation assays as in (*A*) for GIST882 cells after 6 days of treatment. —◆—, 17-AAG only; —■—, 17-AAG + 100nM IM; - -▲- -, 17-AAG + 1000nM IM.

lines. PI3K/AKT activation has been implicated as a crucial KIT oncogenic signaling mechanism (12); thus, we evaluated HSP90 effects on KIT and PI3K interactions after GIST cell treatment with 17-AAG. HSP90 inhibition resulted in disruption of KIT complexing with the regulatory (p85) and catalytic (p110α) PI3K subunits (Fig. 2). These findings are in keeping with the known binding of PI3K proteins to activated KIT (33).

Physical interactions between KIT and HSP90 have not been examined in detail, and it is therefore unclear whether certain KIT imatinib resistance mutations might interfere with HSP90 binding and, thus, with HSP90 chaperone functions. However, it is likely that imatinib-resistant KIT mutations destabilizing HSP90 interactions would be selected against, and seldom encountered, because their interference with HSP90 chaperone activity would result in substantial degradation of the KIT oncoproteins. Our data suggest that the general consequences of HSP90 inhibition in imatinib-resistant GIST cell lines are similar to those previously reported in imatinib-resistant mastocytosis (34). In particular, 17-AAG treatment resulted in dissociation of HSP90 from KIT (Fig. 2) and increased interactions between HSP70 and KIT (Fig. 3), consistent with accepted models of HSP90 client stabilization (16, 17).

To evaluate the dynamics of HSP90 inhibition, we did time course studies of 17-AAG effects on KIT activation, KIT interactions with PI3K, and KIT degradation. Notably, 17-AAG inhibition of KIT activation preceded demonstrable KIT degradation (Fig. 3*A*). Whereas phospho-KIT was completely inhibited after 60 minutes, KIT degradation was undetectable at 60 minutes and 30% of baseline KIT expression persisted at 6 and 24 hours (Figs. 3*A* and 4*A*). Therefore, we hypothesize that HSP90 chaperone

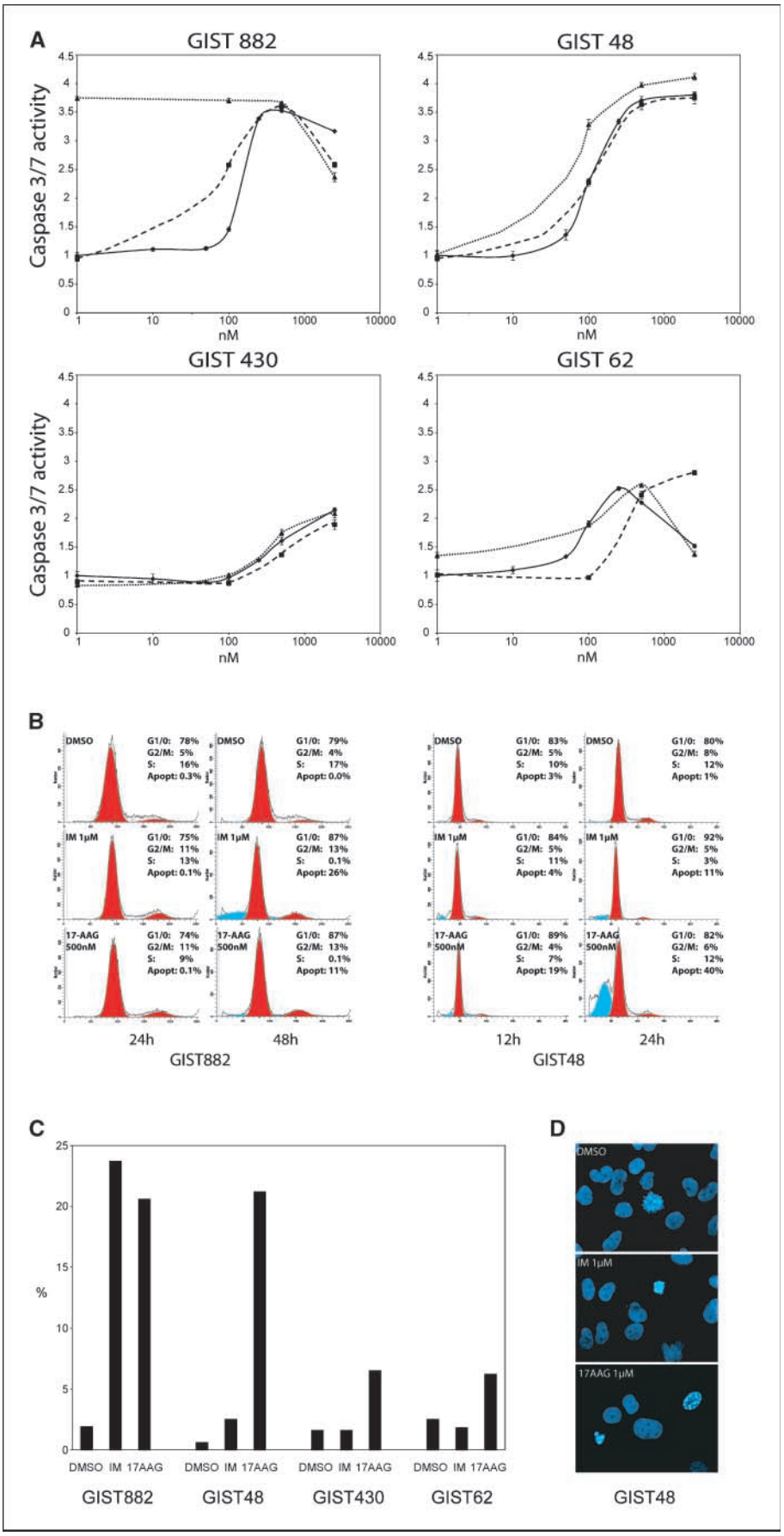

Figure 6. *A,* Caspase-Glo luminescence assay for caspase-3 and caspase-7 activity in imatinib-sensitive (GIST882) and imatinib-resistant GIST cell lines after treatment with 17-AAG alone versus 17-AAG in combination with 0.1 or 1 μmol/L imatinib. Cells were treated for either 24 hours (GIST48, GIST430, and GIST62) or 48 hours (GIST882). The data were normalized to DMSO-only controls. *Points,* mean of quadruplicate cultures; *bars,* SD. —◆—, 17-AAG only; —■—, 17-AAG + 100nM IM; --▲--, 17-AAG + 1000nM IM. *B,* flow cytometry analyses in GIST882 and GIST48 after treatment with 0.5 μmol/L 17-AAG or 1 μmol/L imatinib. *C,* nuclear fragmentation counts after 48-hour treatment with DMSO/control, imatinib, and 17-AAG. Imatinib treatment induced marked nuclear fragmentation only in the imatinib-sensitive cell line, GIST882, although some nuclear fragmentation was also seen in the imatinib-resistant GIST48. 17-AAG treatment induced nuclear fragmentation in all GIST cell lines. *D,* representative DAPI images for the imatinib-resistant GIST48 show a mitotic figure in the DMSO/control culture, an apoptotic pyknotic nucleus in the imatinib-treated culture, and substantially inhibited cell growth with two apoptotic nuclei in the 17-AAG-treated culture.

functions are crucial for stabilization of activated KIT, but only a minor subset of the overall oncogenic KIT proteins are activated at any point in time. KIT and PI3K interactions were only slightly inhibited after 60 minutes of 17-AAG treatment, despite complete inactivation of KIT (Fig. 3*A*). Indeed, complexing between KIT and PI3K was demonstrable after 6 hours of 5 μmol/L 17-AAG treatment (Fig. 2), suggesting that, in GISTs, complexing between KIT and PI3K is not entirely dependent on KIT tyrosine phosphorylation.

We detected no demonstrable increase in KIT ubiquitinylation (Fig. 3) within 60 minutes after 17-AAG treatment, despite that HSP90 inhibition would be expected to promote degradation of activated KIT via ubiquitin-mediated proteasome pathways. This finding is surprising in that FLT3 mutants, closely related to the KIT oncoproteins in GIST, undergo increased ubiquitinylation after 17-AAG treatment (35). However, in our studies, after 6 hours of HSP90 inhibition, KIT ubiquitination decreased to 30% of baseline levels, in parallel with a similar reduction in total KIT expression, consistent with no net change in ubiquitinylation per KIT molecule. These findings might be explained by high baseline levels of KIT synthesis and degradation, with HSP90-regulated KIT ubiquitin fluctuations being functionally meaningful but difficult to show by immunoblotting. Alternatively, KIT degradation resulting from HSP90 inhibition in GISTs might be ubiquitin independent. In this regard, many oncogenic receptor tyrosine kinases have gain-of-function mutations that interfere with Cbl binding, and thereby presumably with ubiquitination (36). For example, Cho et al. (37) recently showed that oncogenic fibroblast growth factor receptor-3 mutations increased fibroblast growth factor receptor-3 stability by interfering with c-Cbl-mediated ubiquitination. In contrast, wild-type KIT is degraded rapidly after ligand activation: in myeloid cells, SCF stimulation results in KIT multiubiquitinylation within 2 to 5 minutes, followed by internalization of the SCF-KIT complex, and near complete loss of KIT expression within 60 minutes ($t_{1/2}$, 20 minutes; ref. 38). In the studies reported herein, we find similar dynamics for degradation of ligand-activated wild-type KIT in the sarcoma cell context. Namely, SCF treatment induced rapid phosphorylation of wild-type KIT, as well as downstream AKT, in Ewing's sarcoma cells, followed by complete KIT degradation within 30 minutes (Fig. 4*B* and *C*). These findings show the efficient nature of the negative control machinery in sarcoma cells, which serves as a check balance to physiologic (wild-type) KIT activation. Further studies are needed to explain the inefficient KIT oncoprotein degradation seen after HSP90 inhibition in GISTs, relative to that seen after wild-type KIT activation by SCF in Ewing's sarcoma. One possibility is that only a small subset of the KIT oncoproteins in GIST cells are dimerized, and phosphorylated, at any point in time, whereas SCF treatment of the Ewing's sarcoma cells might have resulted in nearly universal activation of the wild-type KIT in those cells. Another possibility is that activated KIT oncoproteins in GISTs, even when dechaperoned by HSP90 inhibition, are not ubiquitinated and degraded as rapidly as activated wild-type KIT.

Our studies in the Ewing's sarcoma also highlight the selectivity of HSP90 inhibitors for activated KIT. After 6 hours of HSP90 inhibition, total KIT expression in GIST882 and Ewing's sarcoma (EWS502) cells was decreased by 70% and 20%, respectively (Fig. 4*A*). These studies suggest that clinical use of HSP90 inhibitors will substantially decrease KIT expression in GIST cells, while having lesser effects on KIT-dependent normal cell lineages, including hematopoietic progenitor cells, mast cells, melanocytes, primordial germ cells, and interstitial cells of Cajal. Our attempts to evaluate HSP90 regulation of ligand-activated wild-type KIT were stymied by the rapid degradation of KIT after SCF treatment (Fig. 4). Similar observations were reported by Fumo et al. in Cos-7 cells transfected with wild-type versus mutant *KIT* constructs after SCF and 17-AAG treatment. In the Cos-7 studies, dramatic deregulation of wild-type KIT was seen after SCF and 17-AAG treatment, suggesting that HSP90 had stabilized the activated wild-type KIT. However, a control arm with SCF treatment alone was not shown, and our Ewing's sarcoma studies suggest that SCF induces dramatic and rapid degradation of wild-type KIT, with or without concurrent HSP90 inhibition by 17-AAG (Fig. 4*B*). Using the same experimental conditions as reported by Fumo et al. (SCF pretreatment for 30 minutes, followed by 17-AAG treatment for 6 hours), treatment with 100 ng/mL SCF alone resulted in 90% reduction of total KIT expression (Fig. 4*C*), with or without 17-AAG treatment. Therefore, whereas Fumo concluded that wild-type activated KIT was rapidly degraded after HSP90 inhibition, our findings show these phenomena can be attributed to SCF-mediated KIT degradation alone. Of note, phase I trials of 17-AAG in patients with advanced solid malignancies have reported few grade 3 and grade 4 bone marrow toxicities, consistent with acceptable toxicity in KIT-positive hematopoietic progenitor cells (39–41).

The proliferation assays reported herein underscore that HSP90 inhibition is effective in imatinib-resistant KIT-positive GIST cell lines. IC_{50}s for cell proliferation, after 3 days of 17-AAG treatment, were 130 and 220 nmol/L in the imatinib-resistant GIST48 and GIST430 cell lines, respectively, compared with 3,300 nmol/L in the imatinib-sensitive GIST882. These findings are notable because pharmacokinetic studies have shown that serum levels of 17-AAG (and its active metabolite, 17-AG) of $\geq$1 μmol/L can be maintained over a period of 24 hours in patients (39–41). Notably, 17-AAG antiproliferative properties in GIST882 were lower than those seen after imatinib treatment when comparing 17-AAG and imatinib doses that gave comparable inhibition of the KIT oncoprotein in these cells. These observations suggest that HSP90 chaperones proapoptotic or antiproliferative proteins in the GIST882 cells, with degradation of such proteins countering the effects of KIT oncoprotein inhibition. Slight additive effects between 17-AAG and imatinib were seen when the imatinib-resistant GIST430 and GIST48 were treated with 17-AAG (either 100 nmol/L or 1 μmol/L) together with 100 nmol/L imatinib. However, antagonistic effects were seen with the combination of 100 nmol/L 17-AAG and 1 μmol/L imatinib. Similar antagonistic findings were reported by Radujkovic et al. (42) in imatinib-sensitive chronic myelogenous leukemia (CML) cells whereas additive effects were seen in imatinib-resistant CML cells, possibly resulting from down-regulation of P-glycoprotein by 17-AAG and resultant increased sensitivity to imatinib. In our studies, the mild antagonistic effects between 17-AAG and imatinib were seen at the 3-day time point, but not at 6 days, emphasizing the somewhat idiosyncratic nature of these *in vitro* models. The biological mechanisms of this antagonism are unknown but, as one possibility, could result from inhibition of HSP90 chaperoning for one or more proapoptotic or growth-suppressive proteins.

GIST apoptotic responses to HSP90 inhibition were in keeping with those discussed above for GIST cell proliferation. Imatinib treatment induced caspase activation only in GIST882 whereas 17-AAG treatment (250 nmol/L) induced caspase activation in both imatinib-resistant and imatinib-sensitive GIST cells. Flow cytometric evaluations showed nuclear fragmentation in 11% and

40% of GIST882 cells after treatment with imatinib and 17-AAG, respectively. This evidence of greater apoptotic response with 17-AAG than with imatinib was corroborated by microscopic evaluations of nuclear fragmentation, which showed apoptosis after imatinib treatment in GIST882 only whereas 3- to 10-fold more apoptotic nuclei were seen after 17-AAG treatment. 17-AAG apoptotic effects were also seen in GIST62, presumably due to an HSP90 client other than KIT. Cell cycle measurements were hampered by the slow growth and substantial nuclear pleomorphism of the GIST cell lines. However, both imatinib and 17-AAG resulted in a decreased S phase in GIST882 with increased G_1 and G_2 peaks.

In conclusion, our data suggest that HSP90 chaperone functions are crucial to the stabilization of both imatinib-sensitive and imatinib-resistant KIT oncoproteins in GIST. These strongly activated KIT mutants, unlike wild-type KIT, are exquisitely sensitive to HSP90 inhibition. KIT oncogenic mutations are necessary, and even initiating, transforming events in most GISTs and GISTs therefore provide an ideal solid tumor disease model in which to evaluate HSP90 inhibitors. Indeed, our studies show that HSP90 inhibition is a promising strategy to overcome imatinib resistance in GIST.

Acknowledgments

Received 1/16/2006; revised 5/10/2006; accepted 7/11/2006.

Grant support: Fellowship from the Dr. Mildred Scheel Stiftung für Krebsforschung (S. Bauer) and grants from the Life Raft Group and the Cesarini Team for the Pan-Massachusetts Challenge, the Virginia and Daniel K. Ludwig Trust for Cancer Research, the Ronald O. Perelman Fund for Cancer Research, the Stutman GIST Cancer Research Fund, the Rubenstein Foundation, and Leslie's Links.

The costs of publication of this article were defrayed in part by the payment of page charges. This article must therefore be hereby marked *advertisement* in accordance with 18 U.S.C. Section 1734 solely to indicate this fact.

We thank Jerry Call and the Fletcher Lab for valuable discussions and suggestions.

References

1. Dematteo RP, Lewis JJ, Leung D, et al. Two hundred gastrointestinal stromal tumors: recurrence patterns and prognostic factors for survival. Ann Surg 2000;231:51–8.
2. Hirota S, Isozaki K, Moriyama Y, et al. Gain-of-function mutations of c-kit in human gastrointestinal stromal tumors. Science 1998;279:577–80.
3. Heinrich MC, Corless CL, Duensing A, et al. PDGFRA activating mutations in gastrointestinal stromal tumors. Science 2003;299:708–10.
4. Verweij J, Casali PG, Zalcberg J, et al. Progression-free survival in gastrointestinal stromal tumours with high-dose imatinib: randomised trial. Lancet 2004;364:1127–34.
5. Heinrich MC, Corless CL, Demetri GD, et al. Kinase mutations and imatinib response in patients with metastatic gastrointestinal stromal tumor. J Clin Oncol 2003;21:4342–9.
6. Fletcher JA, Corless CL, Dimitrijevic S, et al. Mechanisms of resistance to imatinib mesylate (IM) in advanced gastrointestinal stromal tumor (GIST). Proc Am Soc Clin Oncol 2003;22:3275–7.
7. Wardelmann E, Thomas N, Merkelbach-Bruse S, et al. Acquired resistance to imatinib in gastrointestinal stromal tumours caused by multiple KIT mutations. Lancet Oncol 2005;6:249–51.
8. Shah NP, Nicoll JM, Nagar B, et al. Multiple BCR-ABL kinase domain mutations confer polyclonal resistance to the tyrosine kinase inhibitor imatinib (STI571) in chronic phase and blast crisis chronic myeloid leukemia. Cancer Cell 2002;2:117–25.
9. Desai J, Shankar S, Skubitz KM, et al. Clonal evolution of resistance to imatinib (IM) in patients (pts) with gastrointestinal stromal tumor (GIST): molecular and radiologic evaluation of new lesions (abstract 3010). Proc Am Soc Clin Oncol 2004;23:197.
10. Shah NP, Tran C, Lee FY, et al. Overriding imatinib resistance with a novel ABL kinase inhibitor. Science 2004;305:399–401.
11. Demetri G, Desai J, Fletcher JA, et al. SU11248, a multitargeted tyrosine kinase inhibitor, can overcome imatinib (IM) resistance caused by diverse genomic mechanisms in patients (pts) with metastatic gastrointestinal stromal tumor (GIST). Proc Am Soc Clin Oncol 2004;22:3001.
12. Bauer S, Hubert C, Heinrich MC, et al. KIT hyperactivation in imatinib-resistant GIST: Implications for salvage therapies. Proc Am Soc Clin Oncol 2005;23:A9034.
13. Fumo G, Akin C, Metcalfe DD, Neckers L. 17-Allylamino-17-demethoxygeldanamycin (17-AAG) is effective in down-regulating mutated, constitutively activated KIT protein in human mast cells. Blood 2004;103:1078–84.
14. BeBoer C, Dietz A. The description and antibiotic production of Streptomyces hygroscopicus var. Geldanus. J Antibiot (Tokyo) 1976;29:1182–8.
15. Schulte TW, Neckers LM. The benzoquinone ansamycin 17-allylamino-17-demethoxygeldanamycin binds to HSP90 and shares important biologic activities with geldanamycin. Cancer Chemother Pharmacol 1998;42:273–9.
16. Isaacs JS, Xu W, Neckers L. Heat shock protein 90 as a molecular target for cancer therapeutics. Cancer Cell 2003;3:213–7.
17. Kamal A, Boehm MF, Burrows FJ. Therapeutic and diagnostic implications of Hsp90 activation. Trends Mol Med 2004;10:283–90.
18. Csermely P, Schnaider T, Soti C, Prohaszka Z, Nardai G. The 90-kDa molecular chaperone family: structure, function, and clinical applications. A comprehensive review. Pharmacol Ther 1998;79:129–68.
19. Solit DB, Scher HI, Rosen N. Hsp90 as a therapeutic target in prostate cancer. Semin Oncol 2003;30:709–16.
20. Munster PN, Basso A, Solit D, Norton L, Rosen N. Modulation of Hsp90 function by ansamycins sensitizes breast cancer cells to chemotherapy-induced apoptosis in an RB- and schedule-dependent manner. Clin Cancer Res 2001;7:2228–36. [See: Sausville EA. Combining cytotoxics and 17-allylamino, 17-demethoxygeldanamycin: sequence and tumor biology matters. Clin Cancer Res 2001;7:2155–8.]
21. Blagosklonny MV, Fojo T, Bhalla KN, et al. The Hsp90 inhibitor geldanamycin selectively sensitizes Bcr-Abl-expressing leukemia cells to cytotoxic chemotherapy. Leukemia 2001;15:1537–43.
22. Munster PN, Srethapakdi M, Moasser MM, Rosen N. Inhibition of heat shock protein 90 function by ansamycins causes the morphological and functional differentiation of breast cancer cells. Cancer Res 2001;61:2945–52.
23. Sausville EA, Tomaszewski JE, Ivy P. Clinical development of 17-allylamino, 17-demethoxygeldanamycin. Curr Cancer Drug Targets 2003;3:377–83.
24. Tuveson DA, Willis NA, Jacks T, et al. STI571 inactivation of the gastrointestinal stromal tumor c-KIT oncoprotein: biological and clinical implications. Oncogene 2001;20:5054–8.
25. Crouch SP, Kozlowski R, Slater KJ, Fletcher J. The use of ATP bioluminescence as a measure of cell proliferation and cytotoxicity. J Immunol Methods 1993;160:81–8.
26. Garcia-Calvo M, Peterson EP, Leiting B, et al. Inhibition of human caspases by peptide-based and macromolecular inhibitors. J Biol Chem 1998;273:32608–13.
27. Karvinen J, Hurskainen P, Gopalakrishnan S, et al. Homogeneous time-resolved fluorescence quenching assay (LANCE) for caspase-3. J Biomol Screen 2002;7:223–31.
28. Choi Y, Ta M, Atouf F, Lumelsky N. Adult pancreas generates multipotent stem cells and pancreatic and nonpancreatic progeny. Stem Cells 2004;22:1070–84.
29. Duensing A, Medeiros F, McConarty B, et al. Mechanisms of oncogenic KIT signal transduction in primary gastrointestinal stromal tumors (GISTs). Oncogene 2004;23:3999–4006.
30. Rubin BP, Singer S, Tsao C, et al. KIT activation is a ubiquitous feature of gastrointestinal stromal tumors. Cancer Res 2001;61:8118–21.
31. Corless CL, McGreevey L, Haley A, Town A, Heinrich MC. KIT mutations are common in incidental gastrointestinal stromal tumors one centimeter or less in size. Am J Pathol 2002;160:1567–72.
32. Oosterom AT, Dumez H, Desai J, et al. Combination signal transduction inhibition: A phase I/II trial of the oral mTOR-inhibitor everolimus (E, RAD001) and imatinib mesylate (IM) in patients (pts) with gastrointestinal stromal tumor (GIST) refractory to IM. Proc Am Soc Clin Oncol 2004;24:3002.
33. Linnekin D. Early signaling pathways activated by c-Kit in hematopoietic cells. Int J Biochem Cell Biol 1999;31:1053–74.
34. An WG, Schulte TW, Neckers LM. The heat shock protein 90 antagonist geldanamycin alters chaperone association with p210bcr-abl and v-src proteins before their degradation by the proteasome. Cell Growth Differ 2000;11:355–60.
35. George P, Bali P, Cohen P, et al. Cotreatment with 17-allylamino-demethoxygeldanamycin and FLT-3 kinase inhibitor PKC412 is highly effective against human acute myelogenous leukemia cells with mutant FLT-3. Cancer Res 2004;64:3645–52.
36. Peschard P, Park M. Escape from Cbl-mediated down-regulation: a recurrent theme for oncogenic deregulation of receptor tyrosine kinases. Cancer Cell 2003;3:519–23.
37. Cho JY, Guo C, Torello M, et al. Defective lysosomal targeting of activated fibroblast growth factor receptor 3 in achondroplasia. Proc Natl Acad Sci U S A 2004;101:609–14.
38. Miyazawa K, Toyama K, Gotoh A, et al. Ligand-dependent polyubiquitination of c-kit gene product: a possible mechanism of receptor down-modulation in M07e cells. Blood 1994;83:137–45.
39. Goetz MP, Toft D, Reid J, et al. Phase I trial of 17-allylamino-17-demethoxygeldanamycin in patients with advanced cancer. J Clin Oncol 2005;23:1078–87.
40. Grem JL, Morrison G, Guo XD, et al. Phase I and pharmacologic study of 17-(allylamino)-17-demethoxygeldanamycin in adult patients with solid tumors. J Clin Oncol 2005;23:1885–93.
41. Banerji U, O'Donnell A, Scurr M, et al. Phase I pharmacokinetic and pharmacodynamic study of 17-allylamino, 17-demethoxygeldanamycin in patients with advanced malignancies. J Clin Oncol 2005;23:4152–61.
42. Radujkovic A, Schad M, Topaly J, et al. Synergistic activity of imatinib and 17-AAG in imatinib-resistant CML cells overexpressing BCR-ABL-Inhibition of P-glycoprotein function by 17-AAG. Leukemia 2005;19:1198–206.

Heat Shock Protein 90 Inhibition in Imatinib-Resistant Gastrointestinal Stromal Tumor

Sebastian Bauer, Lynn K. Yu, George D. Demetri, et al.

Cancer Res 2006;66:9153-9161.